

Studying Interseismic Deformation Using InSAR Phase-gradient Stacking: Application to the North Anatolian Fault

Ziming Liu¹ and Teng Wang²

¹Peking University

²Peking University, Nanyang Technological University, Southern Methodist University

November 22, 2022

Abstract

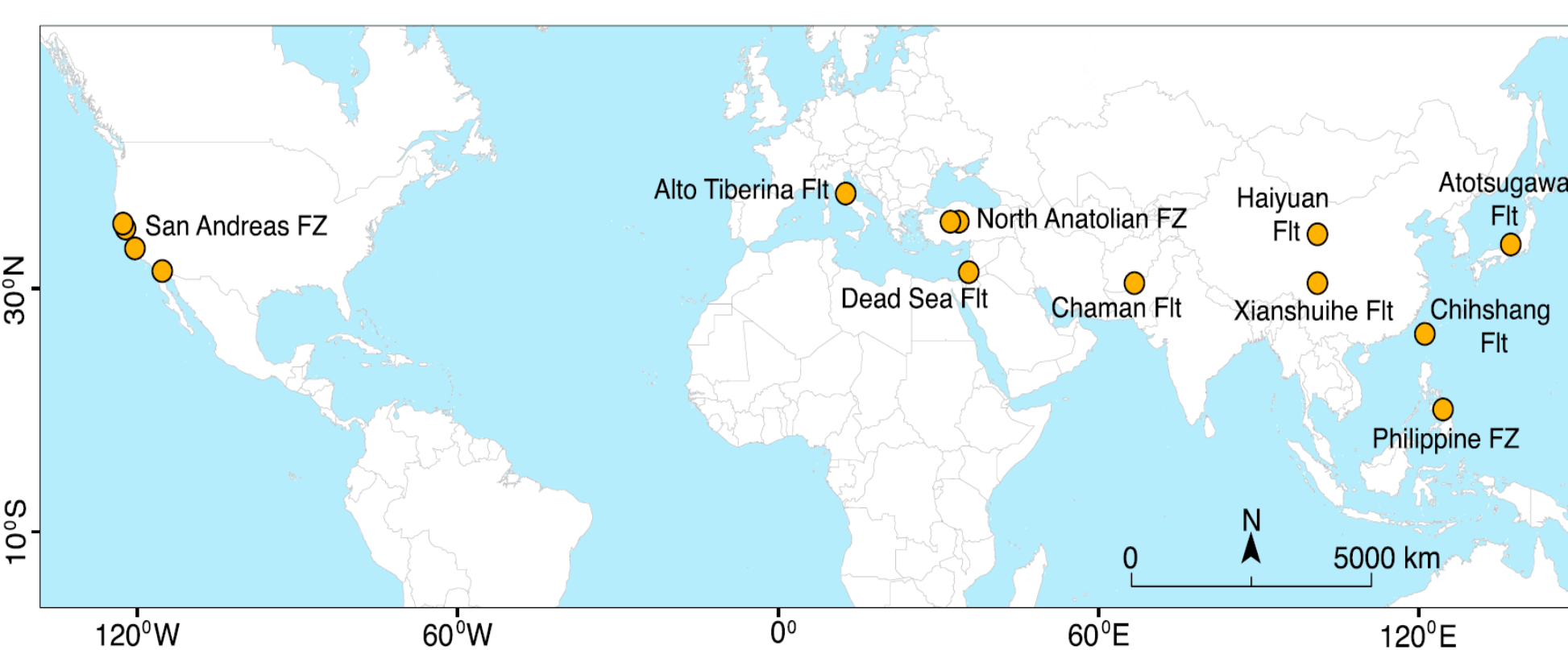
The geodetic measurements of accumulated strains along active faults during their interseismic periods have a strong connection with faulting dynamics and seismic hazards evaluation. InSAR has been widely applied to study the interseismic deformation along active strike-slip faults around the world. However, various limitations such as that from phase unwrapping errors and tropospheric delays are often encountered, hindering our interpretation and model inversion. Phase-gradient stacking is a method that sums up wrapped phase differences of adjacent pixels in multi-interferograms. It has been successfully conducted to reveal local deformation signals across coseismic fractures, yet lacks of application to relatively larger-scale deformation signals. Here we apply the phase-gradient stacking method, for the first time, to study the interseismic deformation along the North Anatolian Fault with Sentinel-1 SAR images acquired from 2014 to 2021. We obtain the strain rate field across the North Anatolian fault without the need of unwrapping hundreds of large interferograms. Segments with surface creep and strong coupling effects can be clearly distinguished in the phase gradient maps, allowing us to directly invert for their long-term slip rates and locking depths. Our preliminary, but promising results show that the phase-gradient stacking method has advantages in studying interseismic deformation along strike-slip faults by directly connecting strain with fault parameters.

Key Points

1. Stacking InSAR phase gradient can study the interseismic strain rate across strike-slip fault
2. The mapped strain rate allows for detecting and mapping creeping segments.
3. Slip rates and locking depths of creeping segments are derived from strain rates.

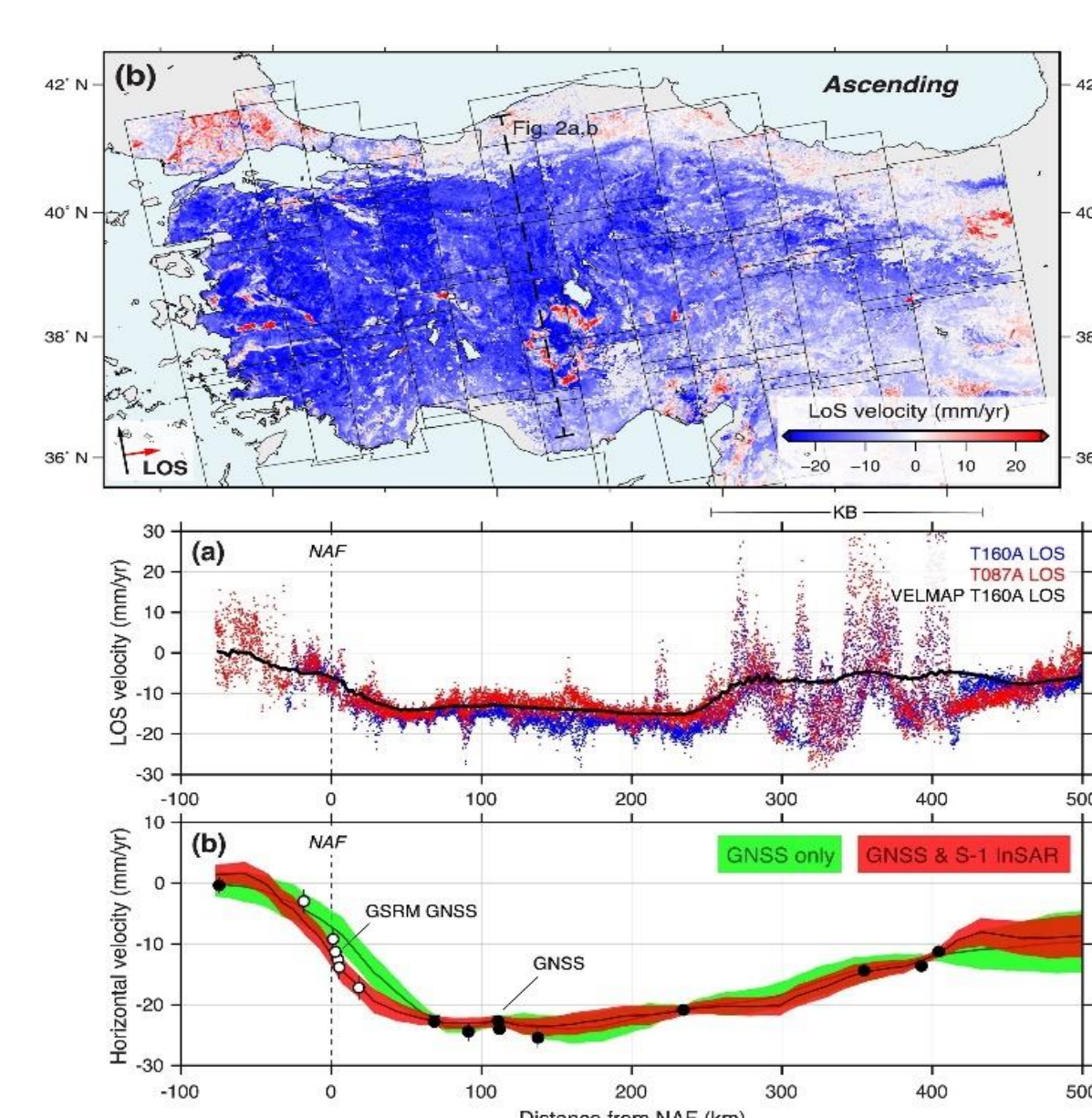
INTRODUCTION

The study of interseismic strains across strike-slip faults plays an important role in understanding the strain accumulation and releasing during earthquake cycles, and the assessment of seismic hazards along fault zones. Because of the steady-state velocity strengthening frictional property, creeping may occur in the uppermost crust for some faults [Kaneko et al., 2013]. Detecting and mapping these creeping segments is important to reveal the frictional heterogeneity along large strike-slip fault system. Previous Interferometric Synthetic Aperture Radar (InSAR) study of the creeping faults is hard to precisely determine the spatial extent of shallow creep from the displacement information. Moreover phase unwrapping are unavoidable, which takes large computational resources and introduces 2π phase errors. Here, We propose the phase-gradient stacking method to detect and map the creeping segment along the North Anatolian Fault in Turkey.

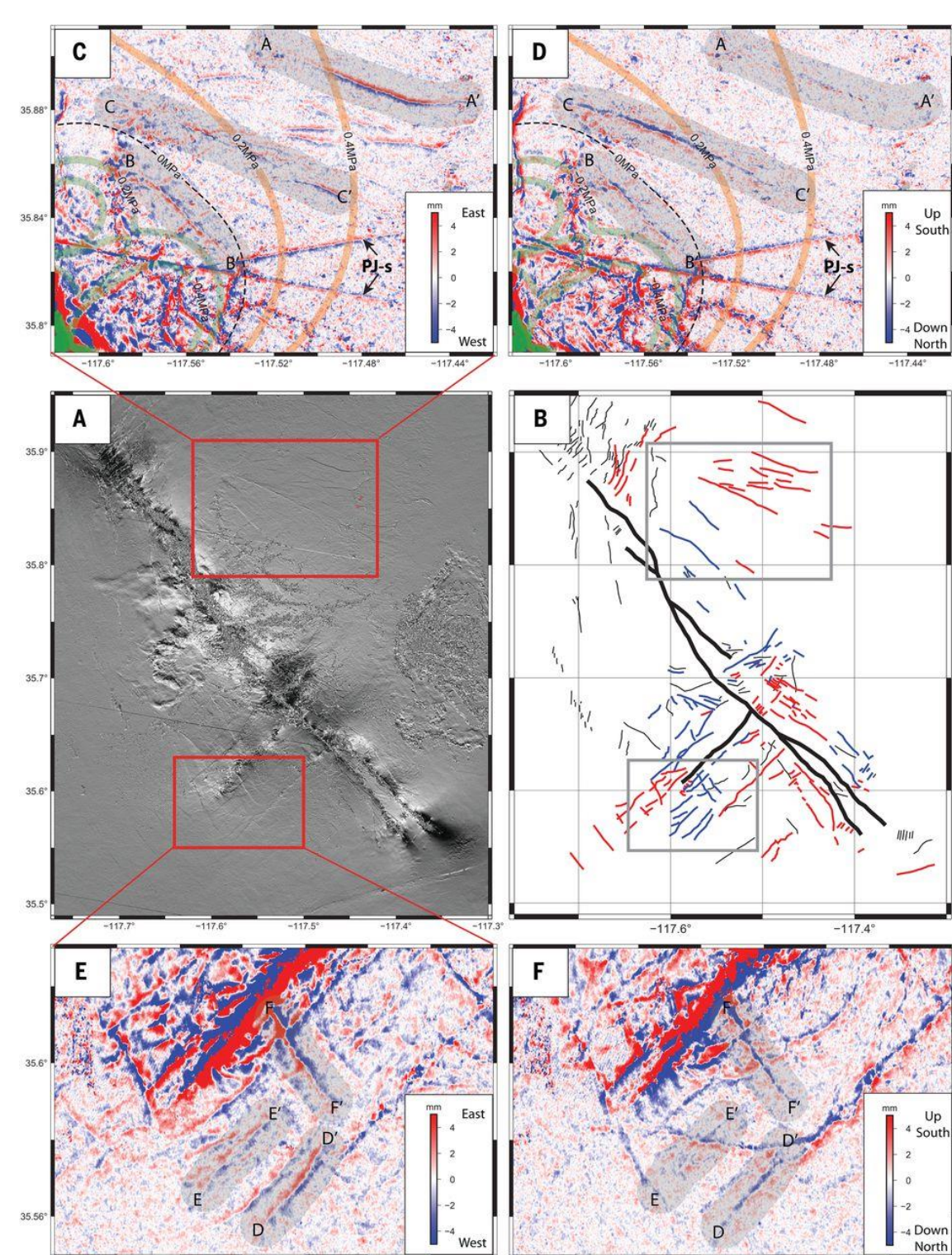


Global view of the locations of the world's well-documented shallow continental creeping faults (circles). [Harris, R. A., 2017]

PREVIOUS STUDY



Weiss et al. (2020) map the deformation field of the whole Anatolia in Turkey. From the bottom profile, the velocity gradient obtained from InSAR & GNSS observation on the Ismetpasa creeping segment is lower than GRSM GNSS indicates. It is difficult to determine the special extent of the creeping segments.



Xu et al. (2020) use the phase gradient method to detect the previously unmapped earthquake fractures.

METHODS

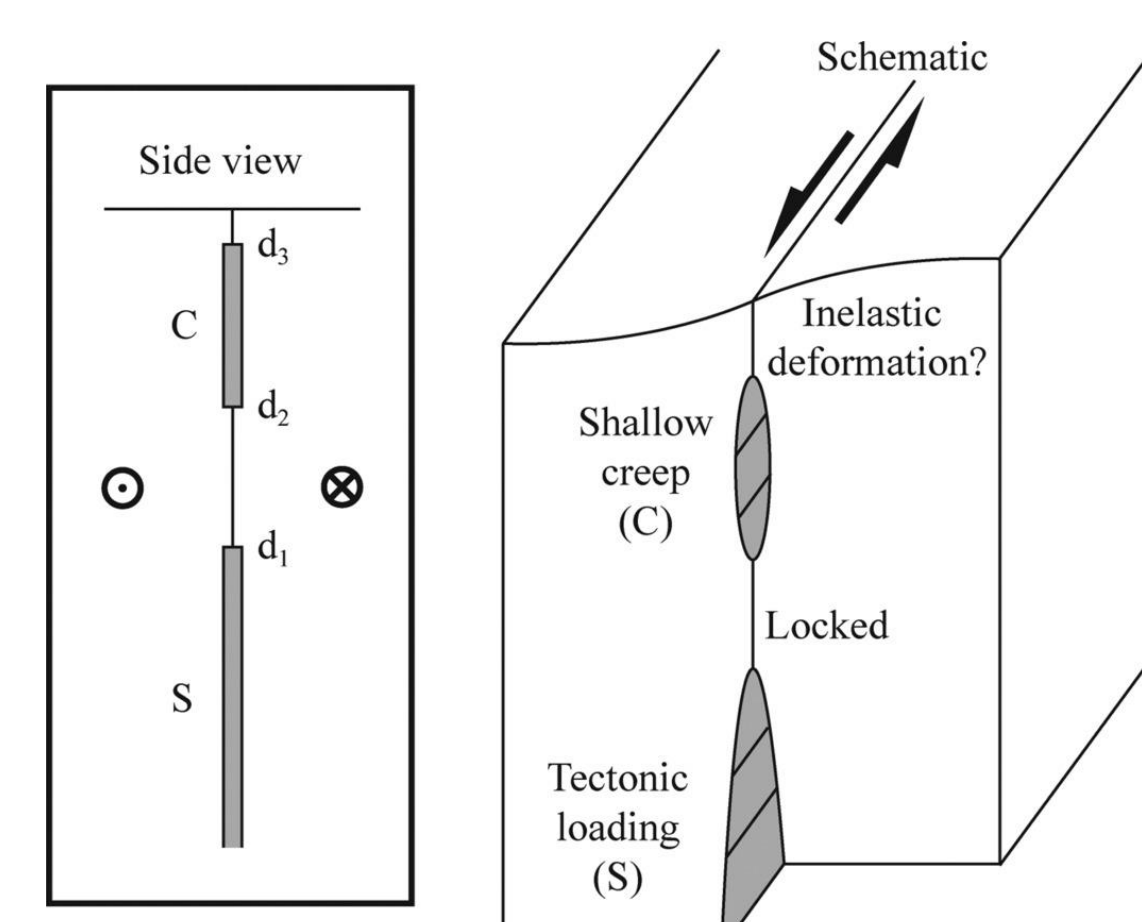
Phase gradient stacking:

We calculated the phase difference of the adjacent pixels for each wrapped interferogram along the NS/EW direction and stacked the gradient images to enhance the signal-to-noise ratio.

$$\sum_{n=1}^N W\{\psi_{i+1,j} - \psi_{i,j}\} = \sum_{n=1}^N (\phi_{i+1,j} - \phi_{i,j})$$

$$\sum_{n=1}^N W\{\psi_{i,j+1} - \psi_{i,j}\} = \sum_{n=1}^N (\phi_{i,j+1} - \phi_{i,j})$$

Forward model of fault creep: 1-D elastic dislocation model:



X. Qiao and Y. Zhou (2021)

Ziming Liu¹ and Teng Wang¹

¹School of Earth and Space Science, Peking University, Beijing, China

For velocity:

$$V_{par}(x) = -\frac{S}{\pi} \arctan\left(\frac{x-\xi_1}{d_1}\right) + \frac{C}{\pi} \left(\arctan\left(\frac{x-\xi_2}{d_2}\right) - \arctan\left(\frac{x-\xi_3}{d_3}\right) \right) + a$$

$$\xi_1 = \frac{d_1}{\tan(\theta_1)}, \xi_2 = \frac{d_2}{\tan(\theta_2)}, \xi_3 = \frac{d_3}{\tan(\theta_3)}$$

For strain rate:

$$S_{par}(x) = -\frac{S}{\pi} \cdot \frac{d_1}{(x-\xi_1)^2 + d_1^2} + \frac{C}{\pi} \left(\frac{d_2}{(x-\xi_2)^2 + d_2^2} - \frac{d_3}{(x-\xi_3)^2 + d_3^2} \right)$$

Inversion Approach: Monte Carlo simulations

To estimate the maximum a posteriori (MAP) solution and corresponding parameter uncertainties. [Qiao, X., & Zhou, Y., 2021]

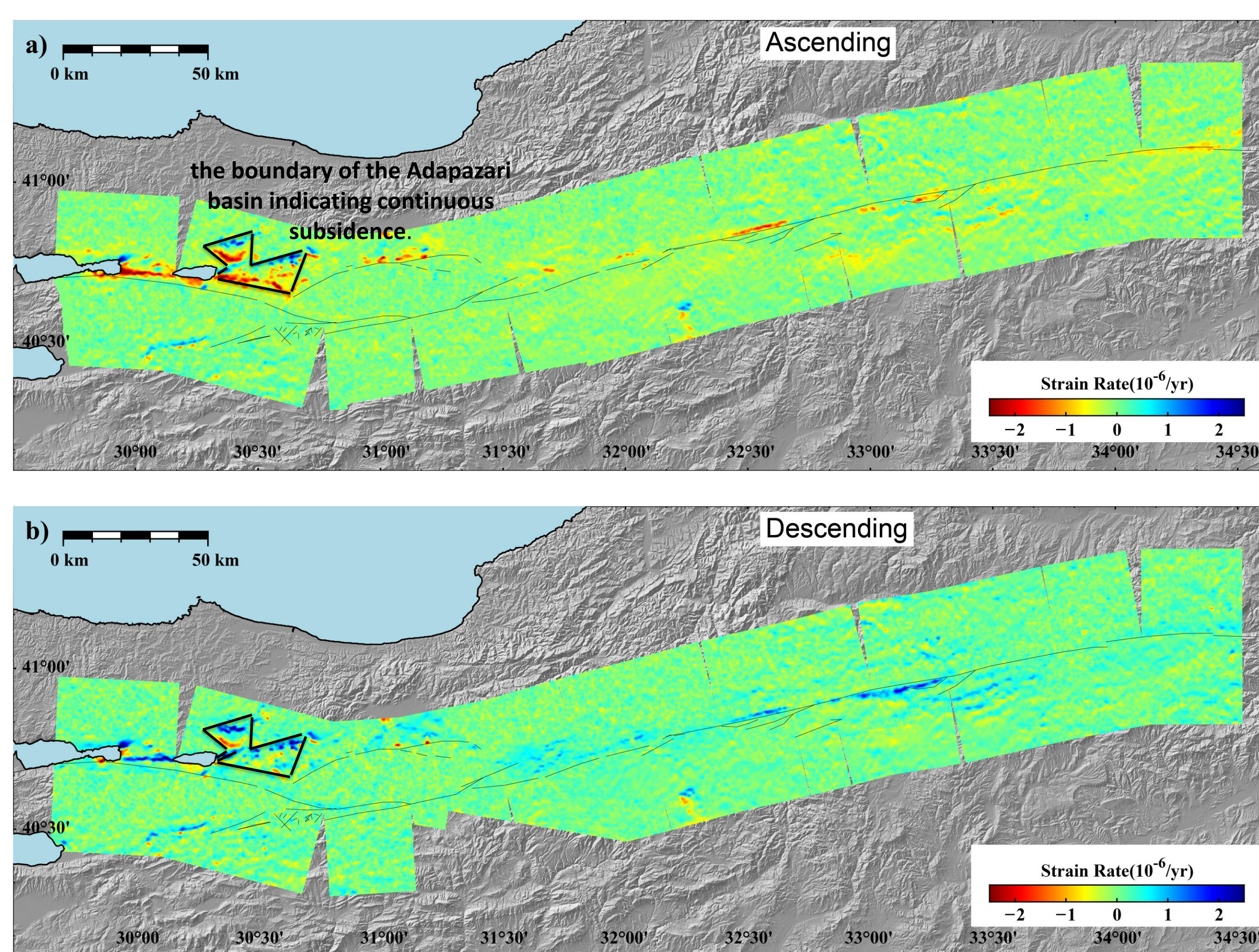
SAR DATA SET

We applied our method to map the creeping segments along the North Anatolian Fault (NAF). We processed Sentinel-1 S1A/B images acquired since 2014, covering the west and central part of the NAF including two well-known creeping segments.

Table :Sentenal-1 data set

	Track 160	Track 87	Track 138	Track 65	Track 167
Direction	Ascending	Ascending	Descending	Descending	Descending
Baseline	1/2/3 years				
Time span	2014/10/04-2021/08/22	2016/06/02-2021/03/08	2014/10/15-2021/08/21	2014/10/10-2021/03/13	2015/08/25-2021/02/24
Independent observations	222	141	158	142	180
Interferograms	323	235	210	203	224
Avg. coherence	0.1454	0.1869	0.1796	0.1722	0.1834

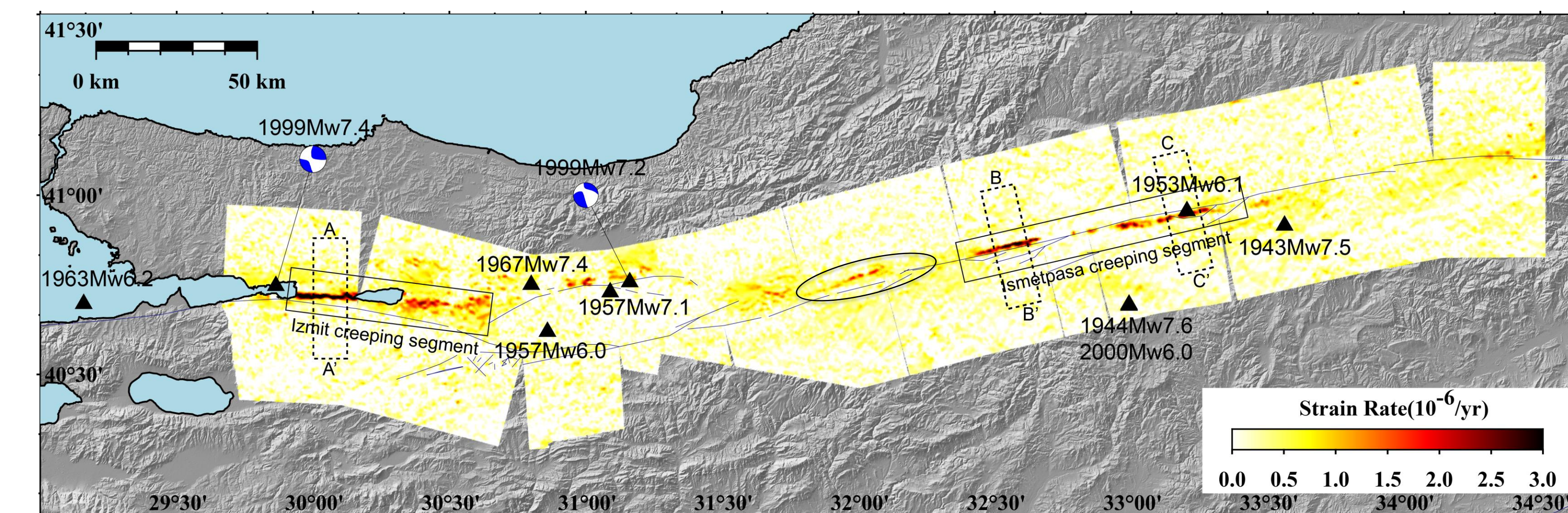
RESULT



LOS velocity gradient rate along north-south direction from (a) ascending tracks and (b) descending tracks.

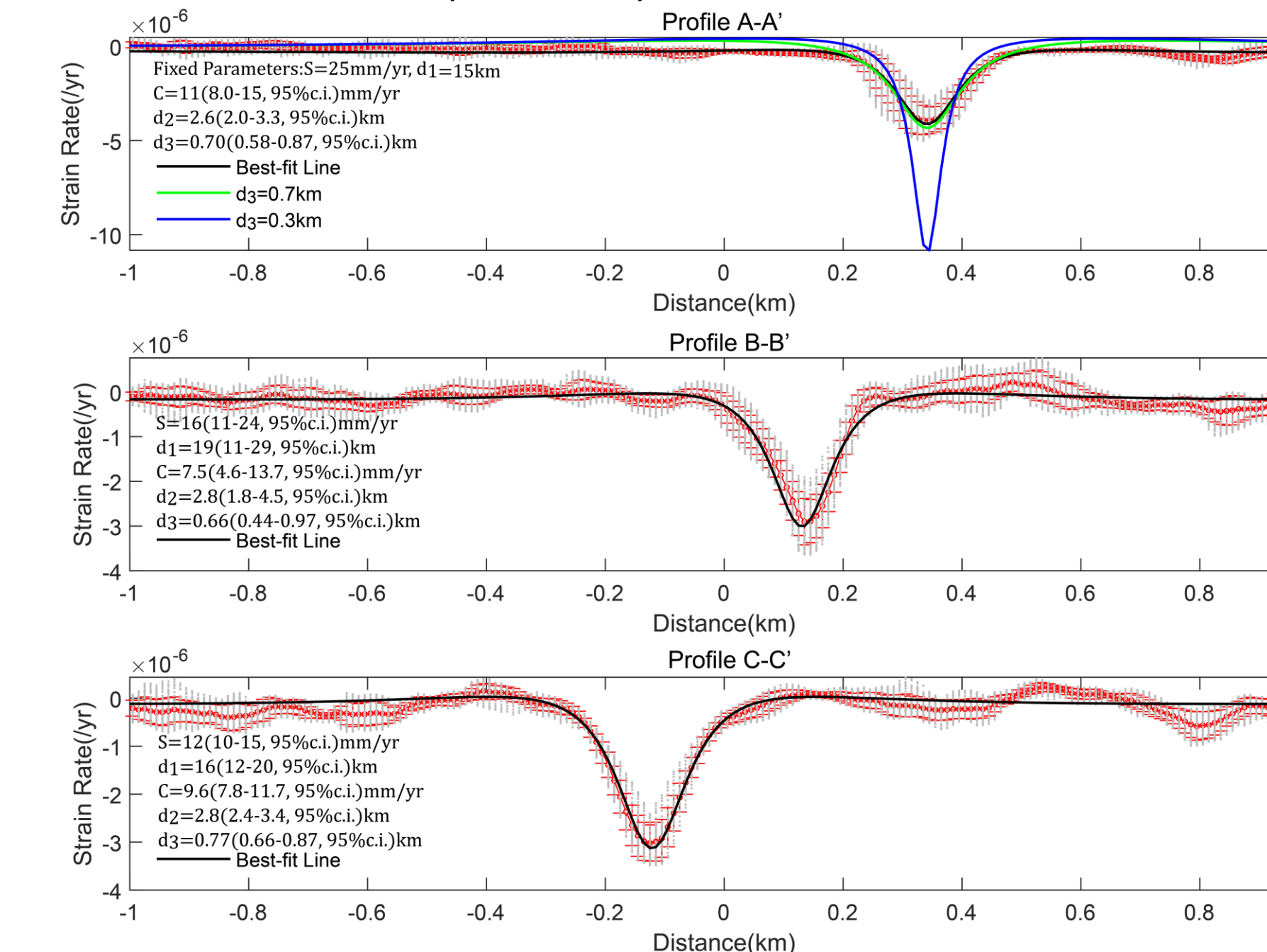
With the assumption that the fault-normal motion is negligible, we can use LOS observations from ascending and descending tracks to obtain the fault-parallel and vertical components.

$$\begin{bmatrix} G_{asd} \\ G_{asc} \end{bmatrix} = \begin{bmatrix} \cos(S - h_{asc} + \frac{\pi}{2}) \sin\theta_{asc} & \cos\theta_{asc} \\ \cos(S - h_{asc} + \frac{\pi}{2}) \sin\theta_{asc} & \cos\theta_{asc} \end{bmatrix} \begin{bmatrix} G_{para} \\ G_{vert} \end{bmatrix}$$

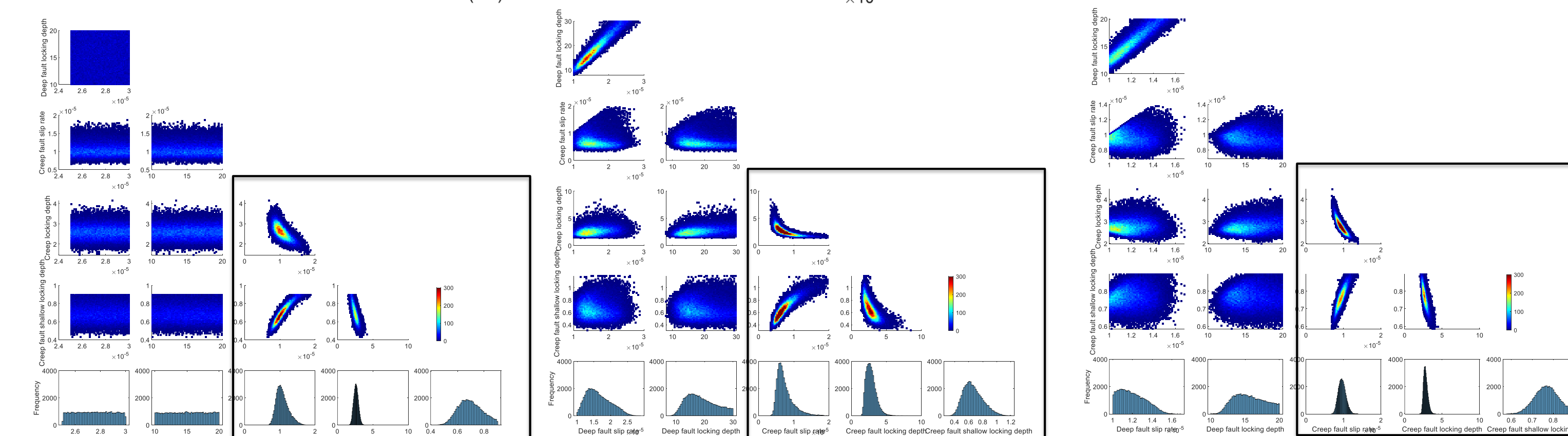


Fault-parallel strain rate indicates the precise location of shallow creeping segments. Black triangles represent the historical earthquakes since 1944. Izmit creeping segment and Ismetpasa creeping segment are shown obviously on the strain rate map. A new creeping segment is detected ~5km north of NAF and ~30 km west of the Ismetpasa segment. (Black ellipse)

In A-A', Green line is strain rate we use parameters from (Hussain et al.,2016) and a shallow creep locking depth with 0.7km (our result), blue line is with 0.3km.



Data parameters and model prediction along Profiles. Black solid line is the model predicted strain rate using the best-fit parameters. Red line with error bar indicates the 1σ data uncertainties. For profile A-A', we fix the deep fault slip rate and locking depth to get a better inversion result. For profile B-B', C-C' (Ismetpasa Creeping Segment), we find the S and d1 are weakly constrained by the original data because the phase gradient method suppresses the long-wavelength signal.



Probability density function (PDF) of five parameters of deep slip rate, locking depth, shallow creep rate, and bottom and top depths of shallow creep for profile A-A', B-B', and C-C'.

DISCUSSION AND CONCLUSIONS

1. The phase-gradient stacking is sensitive to the short wavelength signal, allowing for revealing the accumulated strain rate of the creeping fault. It also provides good resolution for locating the spatial extent of creeping segment. Known creeping segments along NAF, namely the Izmit and Ismetpasa segments exhibit clearly strain localization from the fault-parallel strain map. A possible creeping segment appears ~5km north of NAF, and ~30km west of the Ismetpasa segment.
2. Applying strain into the inversion process is a new attempt for us. Because the model is highly sensitive to the locking depth and exists the trade-off between parameters, the inversion is highly non-unique. Filtering during the InSAR process may have an impact on the strain rate. Also, we introduce the shallow creep locking depth which may not exist in some segments into the inversion to avoid the singularity of the model. However, this parameter can have a large impact on the inversion result. We are still trying to resolve this issue.
3. Compared to previous interseismic deformation studies, phase-gradient stacking owns the ability to detect new creep segments efficiently and accurately without prior information. We can apply this method for searching creeping segments on strike-slip faults on a global scale.

REFERENCE

Hussain, E., Wright, T. J., Walters, R. J., Bekaert, D. P., Lloyd, R., & Hooper, A. (2018). Constant strain accumulation rate between major earthquakes on the North Anatolian Fault. *Nature communications*, 9(1), 1-9.

Hussain, E., Wright, T. J., Walters, R. J., Bekaert, D., Hooper, A., & Houseman, G. A. (2016). Geodetic observations of postseismic creep in the decade after the 1999 Izmit earthquake, Turkey: Implications for a shallow slip deficit. *Journal of Geophysical Research: Solid Earth*, 121(4), 2980-3001.

Kaneko, Y., Fialko, Y., Sandwell, D. T., Tong, X., & Furuya, M. (2013). Interseismic deformation and creep along the central section of the North Anatolian Fault (Turkey): InSAR observations and implications for rate-and-state friction properties. *Journal of Geophysical Research: Solid Earth*, 118(1), 316-331.

Qiao, X., & Zhou, Y. (2021). Geodetic imaging of shallow creep along the Xianshuihe fault and its frictional properties. *Earth and Planetary Science Letters*, 567, 117001.

Weiss, J. R., Walters, R. J., Morishita, Y., Wright, T. J., Lazecky, M., Wang, H., ... & Parsons, B. (2020). High-resolution surface velocities and strain for Anatolia from Sentinel-1 InSAR and GNSS data. *Geophysical Research Letters*, 47(17), e2020GL087376.

Xu, X., Sandwell, D. T., Ward, L. A., Milliner, C. W., Smith-Konter, B. R., Fang, P., & Bock, Y. (2020). Surface deformation associated with fractures near the 2019 Ridgecrest earthquake sequence. *Science*, 370(6516), 605-608.